Cohesion and structure in stage-1 graphite intercalation compounds

D. P. DiVincenzo* and E. J. Mele
Department of Physics and Laboratory for Research on the Structure of Matter, University of Pennsylvania, Philadelphia, Pennsylvania 19104
(Received 23 January 1985)

We have developed a Thomas-Fermi theory for the structural and elastic properties of the first-stage alkali-metal graphite intercalation compounds. We use a simplified model for the electronic structure of these materials which assumes full charge transfer between the alkali metal and the graphite, no hybridization between metal and carbon states, and a uniform distribution of the donated charge on the graphite planes. We have computed lattice constants, compressibilities, shear moduli, alkali-metal diffusion constants and activation energies, and domain-wall thicknesses; general agreement with available experiments is found. These results indicate that our model of the electronic properties is consistent with known elastic and structural properties. The interplane metal-carbon interaction is mostly determined by a competition between Coulomb attraction and hard-core repulsion. The Li ion is much more compact than that of K, Rb, or Cs, which explains the higher compressibility of the Li graphite intercalation compound and the lower Li ionic mobility. The Na—C bond is found to be very soft, explaining the lack of formation of Na-intercalated graphite. The in-plane alkali-metal—alkali-metal interaction is determined almost entirely by the Coulomb interaction, and is thus relatively independent of the alkali-metal species.

I. INTRODUCTION

Recently the structural properties of the first-stage graphite intercalation compounds have received increasing experimental attention.[1,2] Reported in the last few years have been studies of the concentration-temperature and pressure-temperature[3,2] phase diagrams of LiC_6 (Ref. 4) and KC_8 (Ref. 5), investigations of commensurate-incommensurate transitions in the alkali-metal-atom planes,[6,7] measurements of the domain-wall structure in modulated phases,[8] studies of the magnitude and activation energies of alkali-metal diffusivity,[9,10] determination of elastic constants in both the ordered and disordered state, and the measurement of in-plane[11,12] and out-of-plane[13] phonon dispersions. A variety of model studies[14–21] have been done to try to understand some of these phenomena. However, very little effort has been made to correlate this wealth of structural observations with the (presumably known) electronic structure of these solids.

A presently accepted model for obtaining the electronic and structural properties of solids is the density functional theory[22] (DFT) within the local density approximation[23] (LDA). Although this theory has enjoyed considerable success in both describing the energy bands and determining structural energies for a wide variety of metals[24] and semiconductors,[25] it has not been applied extensively to the graphite intercalation compounds. This use of the DFT—LDA approach is presently limited by the immense computational cost of performing calculations on crystals with large unit cells. This means that its application to graphite intercalation compounds has been limited to electronic structure studies of a few of the simplest compounds [LiC_6 (Ref. 26), KC_8 (Refs. 27 and 28), BaC_6 (Ref. 29), and some thin-film studies[30]]. In the future such DFT—LDA studies may be done for a much wider class of compounds.

For the time being we have attempted to obtain a unified understanding of the electronic and structural properties of the graphite intercalation compounds by using a simpler theoretical approach. Our work is also based on the DFT, but within the simpler Thomas-Fermi approximation (TFA) (Ref. 31). The application of the TFA is much less time consuming than the LDA, a simplification which has permitted us to study the systematics of the structural properties of the entire alkali-metal series. The TFA is known to be less accurate than the LDA, but when applied with care it has proved to be capable of producing semiquantitative predictions for the structural properties of a variety of compounds.[32]

We have made predictions about the structural properties of the alkali-metal graphite intercalation compounds by using the TFA along with some simple assumptions about the electronic properties of these materials. These assumptions are the following: (1) Alkali-metal ionization is complete, with full charge transfer to the graphite host. (2) The graphite states may be treated in the rigid-band approximation. These points [especially (1)] continue to be a subject of active investigation;[1,33] recent work[34,35,27,28,26] tends to support the full-ionization picture. In any case, the predictions which we generate using these assumptions are largely consistent with observed structural properties.

Our calculations reproduce the observed trends in properties related to alkali-metal—graphite interactions, e.g., lattice constants and elastic moduli, down the alkali-metal series. We obtain reasonably good predictions for the in-plane diffusion constants of the heavy alkali-metal compounds, and we correctly predict the large enhancement of the activation energy for diffusion in Li-intercalated graphite as compared with the other compounds. In our model the underlying physics which determines these structural properties is quite simple. The intraplanar

carbon—alkali-metal interactions are determined by a competition between the attractive Coulomb and exchange-correlation interactions and hard-core repulsion. As such, this interaction is sensitive to the details of the alkali-metal-ion core (pseudo)potential, and thus Li is found to behave quite differently than K, Rb, or Cs. The Li graphite intercalation compound is unique in that direct C-plane—C-plane interactions play a significant role in stabilizing the crystal. Na has properties which are distinct from any of the other alkali metals. The interplane (pseudo)Coulomb energy for NaC_8 is more repulsive than for the other compounds. As a consequence the Na—C bond is very soft, which seems to be in accord with the observation that Na graphite intercalation compounds do not easily form.[36–38] Later we will account for this behavior in terms of the atomic physics of Na.

In the present model the physics of the in-plane alkali-metal—alkali-metal interaction is even simpler. It is determined almost entirely by classical Coulombic interactions alone, and as such is essentially the same for all the alkali-metal species. The primary difference between the in-plane behavior of the different alkali-metal species comes from changes in the "corrugation potential" generated by the adjoining hexagonal C lattice. This corrugation is much stronger for Li than for the other alkali-metal species, and we predict that discommensurations between locally registered Li domains should be much sharper than for the other metals.

It is important to note that all of these predictions come from a single, simple, unified model which is built directly on our current understanding of the electronic structure of the graphite intercalation compounds. We thus both increase our confidence in our understanding of the electronic structure, and demonstrate the utility of Thomas-Fermi—type approaches for further studies on these materials.

The remainder of this paper is organized as follows. In Sec. II we outline our density-functional approach and its application to the alkali-metal intercalation compounds. Our numerical results for the energetics of these compounds is given in Sec. III: In Sec. III A we explore phenomena related to the alkali-metal—graphite interaction (lattice constants, elastic moduli, diffusion constants); in Sec. III B we study the alkali-metal—alkali-metal interaction, which is relevant to the commensurate-incommensurate transition and domain structure and kinetics. The Appendix gives certain formal results for the Coulomb energy for layered materials which are useful in Sec. III B. Our conclusions are presented in Sec. IV. Preliminary accounts of this work have appeared previously.[39,40]

II. THEORY

In density-functional theory the ground-state energy $E[\rho]$ of the solid is written as a functional of the ground-state electronic charge density ρ of the system. Hohenberg and Kohn[22] proved the existence of an exact functional relationship of this form; long before their work, however, useful empirical theories of the density-functional type were in use.[41,31] In both the original Thomas-Fermi model and the more recent local-density approximations the starting point is our knowledge of the many-body ground-state properties of the uniform electron gas (jellium). The ground-state energy of this system with density ρ_0 and volume Ω is conventionally written

$$E_0(\rho_0)=T_{\rm ni}(\rho_0)+V_C+\rho_0\Omega\epsilon_{\rm xc}(\rho_0). \tag{1}$$

Here $T_{\rm ni}$ is the (kinetic) energy of a *noninteracting* electron gas of the same density ρ_0, and V_C is the classical Coulomb energy ($=0$ for jellium). $\epsilon_{\rm xc}(\rho_0)$, the exchange-correlation energy per particle, is simply the additional term required on the right-hand side of Eq. (1) to give the exact many-body ground-state energy on the right. The function $\epsilon_{\rm xc}$ is known to good accuracy from numerical simulations,[42] and reliable parametrizations of it exist in the literature.[43,44] We have used the Hedin-Lundqvist[43] parametrization. $T_{\rm ni}$ is obviously known exactly, but it can be written in two equivalent ways:

$$T_{\rm ni}=-\sum_i f_i\int_\Omega[\psi_i^0(\mathbf{r})]^*\nabla^2\psi_i^0(\mathbf{r})d\mathbf{r}, \tag{2a}$$

$$=\pi^{4/3}\frac{3^{5/3}}{5}\Omega\rho_0^{5/3}. \tag{2b}$$

Here ψ_i^0 are the one-electron (plane-wave) orbitals, and f_i are the occupation numbers. In this equation and the ones below we use Rydberg atomic units.

The *ansatz* which is made for the density-functional ground-state energy of the inhomogeneous many-body system follows from this knowledge of the homogeneous system. In both the local-density and the Thomas-Fermi approaches the exchange-correlation energy $V_{\rm xc}$ in a system with density $\rho(\mathbf{r})$ is taken to be that of a homogeneous electron gas locally, integrated over all space:

$$V_{\rm xc}[\rho(\mathbf{r})]=\int_\Omega\rho(\mathbf{r})\epsilon_{\rm xc}[\rho(\mathbf{r})]d\mathbf{r}. \tag{3}$$

For the noninteracting kinetic energy there are two possible generalizations, depending on whether the starting point is Eq. (2a) or (2b). In LDA (Ref. 23) the obvious generalization or Eq. (2a) is made:

$$T_{\rm ni}[\rho(\mathbf{r})]=-\sum_i f_i\int_\Omega\psi_i^*(\mathbf{r})\nabla^2\psi_i(\mathbf{r})d\mathbf{r}. \tag{4}$$

That is, the plane-wave eigenstates are replaced by the eigenstates ψ_i of an effective one-particle Schrödinger equation for the inhomogeneous system. In the TFA the starting point is Eq. (2b), and the generalization is the same as the one used for the exchange-correlation energy:

$$T_{\rm ni}[\rho(\mathbf{r})]=\pi^{4/3}\frac{3^{5/3}}{5}\int_\Omega[\rho(\mathbf{r})]^{5/3}d\mathbf{r}. \tag{5}$$

Both approximations for the kinetic energy are justifiable for systems with slowly varying densities; both approximations have been used extensively in systems with rapidly varying densities, for which no rigorous justification exists. Still, both have enjoyed remarkable qualitative and often quantitative success, especially the LDA.[31] Attempts to add correction terms to both $T_{\rm ni}$ and $V_{\rm xc}$ have been made; these terms frequently do not improve the suc-

cess of the theory.[45]

One way of improving the Thomas-Fermi kinetic energy in Eq. (5) which has met with some success involves expressing the kinetic energy in a series of powers of the spatial gradients of the electron density:[31]

$$T=T_{\rm ni}+T^{(1)}[\,|\nabla\rho|^2]+T^{(2)}[\,|\nabla\rho|^4]+\cdots. \tag{6}$$

In practice this does seem to be a convergent series, with $T^{(2)}$ and higher terms contributing only slightly to the total energy. $T^{(1)}$ has been found to be important; it is given by

$$T^{(1)}=\tfrac{1}{36}\int_\Omega \frac{|\nabla\rho(\mathbf{r})|^2}{\rho(\mathbf{r})}d\mathbf{r}. \tag{7}$$

It is found that the inclusion of this term in a Thomas-Fermi model does yield a substantial improvement in predictions of total energies for real systems.[46] We have therefore used this term in the present calculation.

The Coulomb energy of Eq. (1) for an inhomogeneous system is

$$V_C[\rho]=\int_\Omega\int_\Omega \frac{\rho(\mathbf{r}_1)\rho(\mathbf{r}_2)}{|\mathbf{r}_1-\mathbf{r}_2|}d\mathbf{r}_1d\mathbf{r}_2, \tag{8}$$

which is not zero as it is for jellium. In this equation ρ is now understood to contain both the electronic charge density and the charge density of the nucleus. The actual evaluation of this expression requires some care, as has been discussed previously.[47,48] The calculation is simplified somewhat by representing the nucleus and the core electrons by a pseudopotential $V_{\rm ion}$. We have taken $V_{\rm ion}$ to be of the norm-conserving type;[49,50] such potentials are generally angular momentum dependent. In the present application we have used only the $l=0$ part of the pseudopotential and assumed that $V_{\rm ion}$ is local. Within this approximation we can represent the nucleus plus the core electrons by a pseudo-core charge density $\rho_c^P(r)$ which is related to $V_{\rm ion}$ through the Poisson equation

$$\nabla^2V_{\rm ion}(r)=\rho_c^P(r).$$

$\rho_c^P(r)$ varies smoothly in the nuclear region. This representation permits a simple calculation of the core contribution to the Coulomb energy using Eq. (8).

Such a pseudopotential is constructed to describe the cancellation between the large attractive core Coulomb potential and the large repulsive core kinetic energy of the valence orbitals; therefore, we only use the Thomas-Fermi kinetic energy terms of Eqs. (5) and (7) to obtain the kinetic energy of the *valence* electrons. In other words, we evaluate Eqs. (5) and (7) using only the valence charge density ρ_v. Since ρ_v is slowly varying, the use of the Thomas-Fermi approximation should actually be more justifiable than if we had used Eqs. (5) and (7) to evaluate the full kinetic energy, which has a core contribution which varies rapidly in space.

In many applications of norm-conserving pseudopotentials the core contributions to the exchange-correlation energy are also included in $V_{\rm ion}$. However, since $E_{\rm xc}$ is a nonlinear function of ρ (varying roughly like $\rho^{4/3}$), it is not strictly correct to write it as a linear superposition of a core piece plus a valence piece. The error made has been found to be particularly important for alkali-metal atoms, which have fairly weakly bound and extended core states. Therefore we follow the approach of Louie *et al.*[51] and (for the alkali-metal atoms only) exclude the core exchange-correlation energy from $V_{\rm ion}$, but evaluate the full core-plus-valence $V_{\rm xc}$ using Eq. (3). Since ρ_c varies rapidly near the core, the integrand of Eq. (3) has a large number of Fourier components, which is inconvenient for actual calculations. Again following Louie *et al.*, we note that in the integrand

$$V_{\rm xc}\sim(\rho_v+\rho_c)^{4/3} \tag{9}$$

the only important nonlinear contributions occur when $\rho_v\sim\rho_c$. Thus near the nucleus where $\rho_c\gg\rho_v$ we are free to replace ρ_c by a more smoothly varying model-core density ρ_c^M. ρ_c^M is constructed according to

$$\rho_c^M(r)=\begin{cases}A\exp(-r^2/r_W^2), & r<r_0,\\ \rho_c(r), & r>r_0.\end{cases} \tag{10}$$

Here A and r_W are chosen such that the value and slope of ρ_c^M are continuous at r_0, and r_0 is chosen such that $\rho_c(r_0)\gtrsim 2\times\rho_v(r_0)$. Thus ρ_c^M is smoothly varying, its Fourier transform is short ranged, and it is accurate in the region where the nonlinearity in Eq. (9) is important.

With this, the expression we use for the Thomas-Fermi energy in the present work becomes

$$E_{\rm TF}[\rho]=\frac{\pi^{4/3}3^{5/3}}{5}\int_\Omega\rho_v^{5/3}d\mathbf{r}+\tfrac{1}{36}\int_\Omega\frac{|\nabla\rho_v|^2}{\rho_v}d\mathbf{r}+\int_\Omega\int_\Omega\frac{[\rho_c^P(\mathbf{r}_1)+\rho_v(\mathbf{r}_1)][\rho_c^P(\mathbf{r}_2)+\rho_v(\mathbf{r}_2)]}{|\mathbf{r}_1-\mathbf{r}_2|}d\mathbf{r}_1d\mathbf{r}_2$$
$$+\int_\Omega[\rho_c^M(\mathbf{r})+\rho_v(\mathbf{r})]\epsilon_{\rm xc}[\rho_c^M(\mathbf{r})+\rho_v(\mathbf{r})]d\mathbf{r}. \tag{11}$$

Finally, we must specify a procedure for obtaining the valence charge density ρ_v. In a self-consistent Thomas-Fermi calculation, this density would be varied until a functional minimum of the Thomas-Fermi energy is obtained:

$$\frac{\delta E_{\rm TF}}{\delta\rho_v}=0. \tag{12}$$

However, this procedure suffers from the defect that the self-consistent Thomas-Fermi charge density is unlikely to

give an accurate description of the covalent C—C bond in graphite compounds; our semiclassical functional in Eq. (1) should not be expected to describe such a quantum-mechanical bond. Of course, for the most part we are not interested in the C—C in-plane interaction, but rather in the C—C interplane interactions and C—alkali-metal interactions which should be accurately described by Eq. (1). Thus we would be happy to simply freeze-in a correct quantum-mechanical description of the C—C bond charge, not allowing it to vary while we study other more subtle and interesting energetics. To do this we have constructed the valence charge density in a non-self-consistent way which nevertheless retains a good quantum-mechanical description of the covalent-bond charge.

We begin with a quantum-mechanical calculation of the eigenstates of an *isolated* plane of C atoms. (The results of such a LDA calculation have been kindly provided to us by Professor N. A. W. Holzwarth.) If we denote the C-plane wave functions by $\psi^{\text{super}}(\mathbf{k},\mathbf{r})$, then the charge density contributed by the C planes is

$$\rho^{\text{super}}(r)=\int_{E(\mathbf{k})<E_F} |\psi^{\text{super}}(\mathbf{k},\mathbf{r})|^2 d\mathbf{k}. \tag{13}$$

As Eq. (13) suggests, the LDA calculation which we perform is not precisely for an isolated graphite plane, but rather for a supercell of widely spaced graphite planes. The supercell lattice constant a^{super} is about 55% larger than the lattice constant of pure graphite; it was chosen in connection with a study of BaC_6 (Ref. 29). The model which we use for the *isolated* graphite plane is then

$$\rho_{\text{gr}}(\mathbf{r})=\begin{cases}\rho_{\text{super}}(\mathbf{r}), & -a^{\text{super}}/2<z<a^{\text{super}}/2,\\ \rho^{\text{extr}}(\mathbf{r}), & \text{otherwise.}\end{cases}$$

The extrapolation charge density $\rho^{\text{extr}}(\mathbf{r})$ is an exponentially decaying charge which is chosen so that ρ is continuous at $z=\pm a^{\text{super}}/2$ and total charge is conserved. This approximation for $\rho_{\text{gr}}(\mathbf{r})$ has the advantage of being exactly positive definite: $\rho_{\text{gr}}(\mathbf{r})>0$ for all $\mathbf{r}$. The decay constant of the $\mathbf{G}_{||}\neq\mathbf{0}$ components of ρ ($\mathbf{G}_{||}$ is an in-plane reciprocal-lattice vector) are chosen to be 1.3 times as fast as the $\mathbf{G}_{||}=\mathbf{0}$ component; we do this to mimic the known property that corrugations ($\mathbf{G}_{||}\neq\mathbf{0}$) die rapidly away from surfaces. However, there is nothing special about the factor 1.3. We do not expect our final results to be very sensitive to the details of this extrapolation, since $\rho^{\text{extr}}(\mathbf{r})$ is everywhere small.

Thus we complete our construction of the alkali-metal—graphite charge density by a simple linear superposition of the contributions from different graphite planes and alkali-metal atoms. For the case of pure graphite, E_F in Eq. (13) is chosen such that the C planes are electrically neutral. For the alkali-metal graphite intercalation compounds the Fermi energy is raised so that the charge on the C planes compensates the ion charge of the alkali-metal atoms.

This *ansatz* contains several assumptions. First, as discussed in Sec. I, we assume that the alkali-metal atoms are completely ionized, contributing nothing to the valence-charge density but simply donating charge to the graphite planes. This assumption has been rather controversial[1,33] but seems to be supported by recent experiments.[34,35] Second, our charge-density construction does not allow for self-consistent readjustments of the graphite eigenstates due to the presence of the added charge. Since the added charge density [$(\frac{1}{6})e^-$ per C atom] is fairly small on the scale of the total valence-charge density (4 per C atom), this is expected to be only a small effect. (It is indeed found to be a small effect in recent LDA calculations for KC_8.[28]) Third, we have neglected the in-plane polarization of the added charge due to the presence of the positive ions, i.e., we have neglected screening effects. Reference 52 shows that the screening length in graphite is actually anomalously long because of the two dimensionality of the screening and because of the peculiar electronic structure of the host material near the Fermi energy. For most of the cases treated in this paper, therefore, the screening effects will indeed be weak. However, there are cases in which this neglect will cause errors, and we will discuss these cases below.

III. RESULTS

A. Alkali-metal—carbon interactions

In this section we will show results for the total energy [Eq. (1), with the modifications mentioned above], along with its components, the exchange and correlation energy V_{xc}; the electrostatic Coulomb energy V_C; the Thomas-Fermi kinetic energy T_{TF}; and the gradient correction to the kinetic energy $T^{(1)}$. We have computed these as a function of several lattice coordinates of the alkali-metal—graphite lattice: the sandwich spacing c, the position of the alkali-metal superlattice with respect to the graphite lattice τ, and the alkali-metal—alkali-metal separation a. From these we are in a position to discuss various ground-state parameters of the first-stage compounds.

Figures 1 and 2(a)—2(c) show these energies as a function of the carbon-plane separation for the stage-1 alkali-

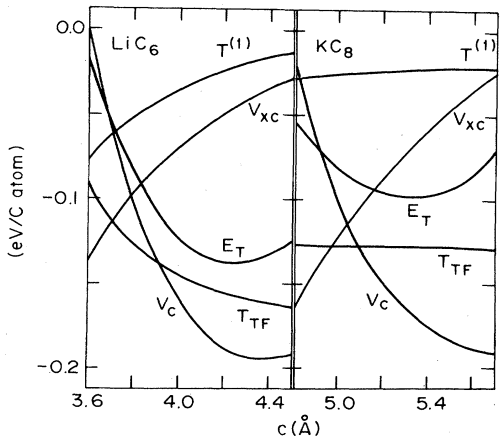

FIG. 1. Total energy E_T and the density-functional energies contributing to it for LiC_6 and KC_8 as a function of the out-of-plane lattice constant c. Energies are in eV/C atom and have been shifted by arbitrary constants.

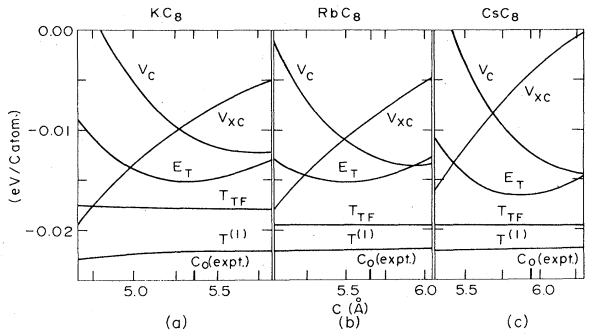

FIG. 2. Same as Fig. 1 for (a) KC_8, (b) RbC_8, and (c) CsC_8. The experimental lattice constant is indicated as c_0.

metal–graphite compounds. Figure 1 compares LiC_6 with KC_8, and Figs. 2(a), 2(b), and 2(c) show KC_8, RbC_8, and CsC_8, respectively. These stoichiometries are the alkali-metal concentrations appropriate for the zero-pressure, low-temperature first-stage phases of these compounds. The Li-intercalated graphite compound differs strikingly from the heavier-alkali-metal graphite intercalation compounds of K, Rb, and Cs, as the figures show. In LiC_6, the general form of the total energy around equilibrium is contributed to dominantly by the electrostatic Coulomb energy, with all the other components of the total energy making roughly equal but small contributions. On the other hand, the general shape of the total-energy curve for the K, Rb, and Cs compounds is determined by a roughly equal contribution from a repulsive Coulomb term and an attractive exchange and correlation term, with the kinetic and gradient terms making essentially no contribution.

First, let us consider the general behavior of the Coulomb contribution. At large lattice constant the Coulomb contribution becomes linear and attractive. This simply represents the attractive force between the alternating positively- and negatively-charged planes in the material. This regime can be seen in Fig. 1 for the case of LiC_6; it occurs at somewhat larger lattice constants than have been plotted for the heavier alkali metals. At smaller lattice constant the Coulomb energy becomes repulsive. This is so because what we call the "Coulomb" energy is actually a pseudo Coulomb energy, that is, it includes contributions from the core kinetic energy which have been folded into the effective ionic pseudopotentials. At small lattice constant the carbon-valence charge begins to penetrate the alkali-metal cores. Thus the core kinetic energy rises, and the effective Coulomb energy becomes repulsive, as is seen for all the curves in Figs. 1 and 2.

The other important contribution to the total energy for most of the first-stage alkali-metal graphite intercalation compounds is the exchange-correlation energy V_{xc}. It is attractive, which (as discussed previously in our work on pure graphite[47]) is generally true for exchange energies. For LiC_6 we have discovered by more detailed analysis that V_{xc} has equal contribution from both the overlap of the C valence charge with the alkali-metal-atom core charge (the nonlinear interaction described above), and from the interaction of valence charge on adjacent C planes. On the other hand, we find that for the heavier alkali metals, only the alkali-metal-atom-core–graphite-valence-charge overlap makes a significant contribution to V_{xc}; that is, there is only negligible direct interaction between adjacent C planes because of the larger lattice constant in the heavier-alkali-metal graphite intercalation compounds as compared with LiC_6. This is the reason that the kinetic energy contributions T_{TF} and $T^{(1)}$ are almost completely flat; in the present formulation of the theory, these energies depend only on adjacent graphite-plane interactions.

Figure 3 shows the results of our calculation for the hypothetical compound NaC_8 as compared again with LiC_6. Na is distinct from all the other alkali metals in that it intercalates into graphite only with considerable difficulty. Some Na-intercalated graphite compounds have been synthesized,[38] and a stage-8 material has been reported.[37] (It was found to have a 2×2 in-plane density.) Low-stage ternary compounds with cointercalated Na and K have been observed.[36] However, no low-stage pure Na graphite intercalation compound has been synthesized. An early model by Hennig[53] based on a Born-Haber cycle involving the work function of graphite and the ionization energy of the alkali metals predicted that the K, Rb, and Cs graphite intercalation compounds would form and the Na graphite intercalation compound would not; however, this model also predicted that the Li graphite intercalation compound would not form, which was later found to be untrue. The lack of formation of Na-intercalated graphite remains a mystery.

The energy curves of Fig. 3 show that NaC_8 is distinct from both LiC_6 and the heavy-alkali-metal MC_8 compounds. The main feature which distinguishes NaC_8 from both LiC_6 and KC_8 is that the (pseudo)Coulomb energy V_C is more repulsive, leading to a flatter E_T near the minimum. We can trace the behavior of V_C back to the atomic physics of the alkali metals. Figure 4 shows the pseudopotentials $V_{ion}(r)$ which we use for Li, Na, and K; they are generated according to the Kerker procedure,[50] with the exchange-correlation correction of Louie *et al.*[51] As the figure shows, the pseudopotential near the origin $V_{ion}(r=0)$ is more repulsive for Na than for either Li or K; this leads to the more steeply rising V_C for NaC_8 in

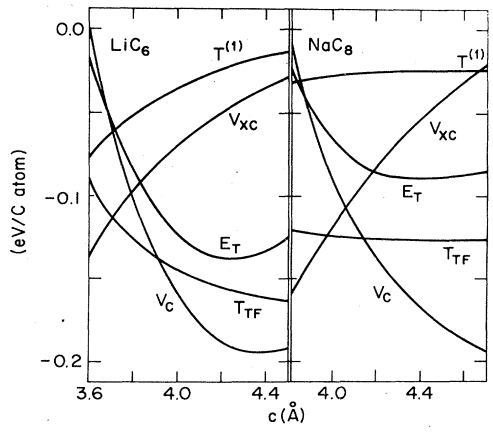

FIG. 3. Comparison of total energy of LiC_6 with the hypothetical compound NaC_8.

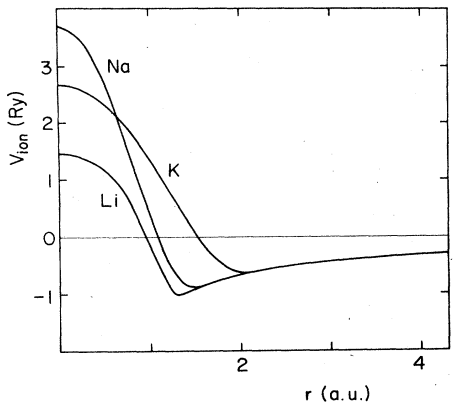

FIG. 4. Ionic pseudopotentials used for Li, Na, and K. The Na potential is more repulsive near the origin, resulting in the more repulsive Coulomb energy V_C of NaC_8 and the flatter E_T.

Fig. 4. This anomaly in $V_{ion}(0)$ is simply a reflection of an anomaly in the Wigner-Seitz radius r_{WS} of the alkali metals. (We take r_{WS} to be defined by the last extremum of the wave function of the outermost s electron.[54]) The Wigner-Seitz volume V_{WS} for Na, rather than being midway between those of Li and K, is nearly the same as for Li; the change of V_{WS} in going from Li→Na→K is in the ratio 15:85. In other words,

$$\frac{V_{WS}(\mathrm{Na})-V_{WS}(\mathrm{Li})}{V_{WS}(\mathrm{K})-V_{WS}(\mathrm{Na})}\approx\frac{15}{85}.$$

This means that the core radius of the Li and Na pseudopotentials is nearly the same, as Fig. 4 shows. On the other hand, the value of the valence s eigenvalue E_s, which determines the strength of the pseudopotential,[55] increases more nearly continuously down the alkali-metal series; the change in E_s in going from Li to K in the sequence Li→Na→K is divided according to the ratio 30:70; i.e.,

$$\frac{E_s(\mathrm{Na})-E_s(\mathrm{Li})}{E_s(\mathrm{K})-E_s(\mathrm{Na})}\approx\frac{30}{70}.$$

Thus the Na pseudopotential, while having about the same extent as Li's, must reproduce a higher s eigenvalue. Therefore, it is more repulsive. The flatness of E_T for NaC_8 resulting from this effect leads to a very low elastic modulus (see below). Since in most materials there is a direct scaling relation between the elastic modulus and the cohesive energy E_{coh},[56] it may be speculated that, although E_{coh} cannot be computed directly in the present work, it is likely to be much smaller for NaC_8 than for the other compounds. This suggests a possible reason for the observed nonformation of NaC_8.

Table I shows the equilibrium lattice constant c_0 as deduced from the minimum of E_T in Figs. 1–3, along with the values obtained from diffraction experiments.[57] Figure 5 also shows these parameters graphically. As the figure demonstrates, we reproduce the trend of the growth of the lattice constant down the alkali-metal series quite reliably. (The experimental Na lattice constant is taken from the C-Na-C sandwich spacing in stage-8 Na-intercalated

TABLE I. Physical parameters for first-stage alkali-metal–graphite compounds.

X	Li	Na	K	Rb	Cs
c_0 (expt.) (Å)[a]	3.70	4.6	5.36	5.66	5.94
c_0 (theor.)	4.42	4.41	5.33	5.52	5.85
$\Delta c/c_0$ (%)	+19.5	−4.0	−0.5	−2.5	−1.5
C_{33} (expt.)[b] (10^{12} dyn/cm^2)	0.88		0.49	0.48	0.64
C_{33} (theor.)	1.39	0.25	1.27	1.29	1.54
E_0^c	0.0	0.0	0.0	0.0	0.0
E_1 (eV)	1.30	0.25	0.18	0.14	0.18
E_1 (expt.)[d]	0.7–1.0		0.1–0.2	0.05–0.10	0.05–0.10
E_2 (eV)	1.60	0.29	0.20	0.16	0.20
C_{44} (expt.)[e] (10^{11} dyn/cm^2)	1.00		0.28		0.30
C_{44} (theor.)	4.00		0.60	0.49	0.67
a_0 (expt.) (Å)	4.26		4.92	4.92	4.92
k_M (eV/Å^2)	0.25		0.26	0.28	0.28
G (eV/Å)	−0.41		−0.87	−1.00	−1.10
k (eV/Å^2)	0.28		0.32	0.35	0.35
l_0 (Å)	6.0		23.0	27.0	24.0
D (expt.)[f] (cm^2/sec)	$\sim 10^{-8}$			5.7×10^{-5}	7.6×10^{-5}
D (theor.)[g]	1.0×10^{-15}		1.0×10^{-5}	2.0×10^{-5}	0.7×10^{-5}

[a]Reference 57.
[b]References 13 and 11.
[c]By convention.
[d]References 9 and 10.
[e]References 11 and 12. Not measured for Rb.
[f]At 523 K. References 9 and 10.
[g]Reference 39.

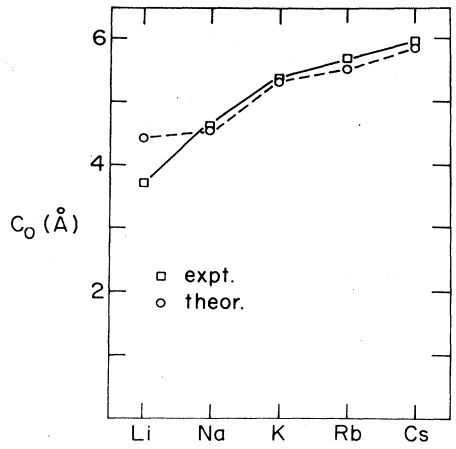

FIG. 5. Experimental and theoretical out-of-plane lattice constants for the first-stage alkali-metal intercalation compounds.

graphite.[37]) The lattice constants of the Na, K, Rb, and Cs graphite intercalation compounds in fact have high quantitative accuracy, being in agreement with experiment to within 4% in each case. We have found that the nonlinear core exchange interaction included in Eqs. (9)—(11) is crucial in obtaining this good agreement; these lattice constants are consistently small by 10—15 % when this effect is not included. It is therefore clear that the nonlinearity of the core exchange interaction is, as Louie *et al.* have noted,[51] essential in describing the energetics of alkali-metal-containing materials.

The result for LiC_6 is different in a number of ways. The agreement between theory and experiment in c_0 is not as quantitatively accurate, although our prediction still follows the general trend quite adequately. [We find that inclusion of the nonlinear core interaction in Eqs. (10) and (11) has virtually no effect on the prediction which our theory makes for the LiC_6 lattice constant.] One possible explanation for this lack of agreement is that our simple charge-density construction, with fully ionized alkali-metal-atom cores, unpolarized graphite π charge, and no carbon-metal hybridization effects, is more realistic for the heavier-alkali-metal graphite intercalation compounds than for LiC_6. Previous speculations[58] have focused on evidence for Li-C hybridization provided by trends in the LiC_6 lattice constant. A theoretical study of the ground-state charge density of LiC_6 has demonstrated the presence of a noticeable hybridization which leads to something resembling a weak covalent bond charge between the Li and C atoms. This theoretical prediction[26,59] has recently been confirmed by Compton scattering measurements.[60] While there is some evidence that this hybridization effect is less pronounced in KC_8, this conclusion remains controversial,[1,33] and other studies have reached the opposite conclusion.[34,35] Still, it is our belief that the neglect of electronic hybridization is likely to be the main source of the quantitative error in our predicted LiC_6 lattice constant.

As implied by the above discussion, we explain the trend of lattice constants through the alkali-metal series by changes in the nature of the core-valence interaction. The greatest difference in the atomic physics between Li and K, Rb, and Cs is the presence of shallow p cores in the latter but not in the former. (We will exclude Na from the present discussion.) The Li core, composed of $1s$ electrons, is about 60 eV below vacuum. Thus the core charge is very compact, its interaction with the carbon π charge is quite short ranged, and the lattice constant is small. In fact we have shown that the LiC_6 lattice constant is stabilized at least as much by C-plane—C-plane interactions as by Li-C interaction. In K, Rb, and Cs, on the other hand, the outer p core lies only 15—20 eV below vacuum, with this energy decreasing down the Periodic Table. The resulting core charge ρ_c^M becomes more and more diffuse, interacts more and more strongly with the C valence charge, and causes the lattice constant to increase down the Periodic Table. This physical picture is perhaps not surprising, given the known fact that the alkali-metal—graphite lattice constants scale consistently with atomic radii.[57] Li's lack of a p core has been noted previously.[58] However, the outer atomic s charge of the alkali metal is apparently playing no detectable role in the determination of the out-of-plane lattice constant, and thus our assumption that it is absent is supported.

The planar compressibility C_{33} is determined from Figs. 1 and 2 through the curvature of E_T at equilibrium. If we fit the total energy as a function of the plane-plane separation c by a parabolic form around equilibrium c_0, $E_T=(1/2)K(c-c_0)^2+E_0$, then the elastic modulus is given by

$$C_{33}=\frac{c_0 K}{A_0}. \tag{14}$$

Here A_0 is the basal plane area per C atom. The values deduced for C_{33} are shown in Table I along with the values obtained by neutron-scattering measurements of longitudinal-acoustic phonons perpendicular to the planes;[11,13] these values are plotted in Fig. 6. (Naturally, no experimental data exist for NaC_8.) For all compounds except NaC_8, these elastic constants are fairly strong, being in the range of typical semiconductor moduli,[61] and they are larger than for pure graphite. The agreement between theory and experiment is on the same order as graphite, with discrepancies of about a factor of 2. It may be that this is the best that may generally be expected with

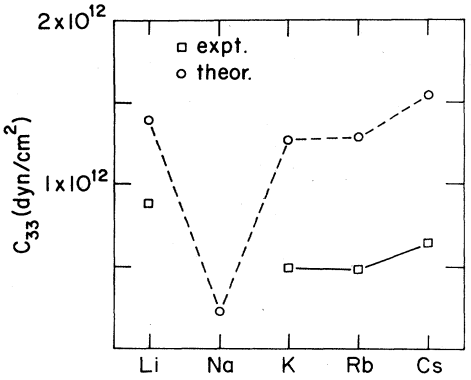

FIG. 6. Same as Fig. 5 for out-of-plane compressional elastic modulus C_{33}. Circles are theory, squares experiment.

the present approximate Thomas-Fermi theory, although previous studies on carefully selected systems[32] have on occasion done better. It is promising that we appear to reproduce the overall trend of C_{33} down the alkali-metal series fairly well. Experimentally the Li compound has a high compressibility, K and Rb are smaller and nearly identical, and Cs is again higher. This is precisely what we obtain from the theory. The greater stiffness of LiC_6 is easy to understand in terms of the greater compactness of the sandwich. Unfortunately we have not been able to find a similar underlying explanation of the heaviest Cs's relatively larger stiffness. As discussed above, Fig. 6 shows that C_{33} for NaC_8 deviates remarkably from that of the other compounds, being about a factor of 5 softer.

As in our study of pure graphite,[47] we are also interested in deformations of the lattice involving shear distortions, motions of the constituents parallel to the basal plane. In the alkali-metal compounds, however, there is a much richer variety of physical properties which are related to these deformations which can be probed experimentally. We are not only interested in the ordinary shear elastic modulus C_{44} but also in the global potential energy surface for the motion of alkali-metal atoms through the corrugated potential produced by the graphite host. From this we will discuss some important physical properties of the alkali-metal layers: the competition of diffusive and harmonic motions, the diffusion times which are relevant to staging transformations or compound formation, and the driving forces for ordered phases, commensurate or incommensurate, within the alkali-metal layer. We will in fact be interested in the same sort of physics as is uncovered in studies of surface adsorption to which TFA theories have also been applied (rare gases on graphite,[62,63] for example); the intercalation problem is different in a number of interesting ways, as will become clear below.

The theoretical method for probing in-plane motion of alkali-metal atoms in the carbon host is very straightforward; we simply displace the entire alkali-metal superlattice in the first-stage compound to different positions relative to the surrounding graphite substrate, and calculate the kinetic and potential contributions to the total energy. Once again, this is done using our simple linear superposition construction for the compound charge density. In each calculation described here the layers are positioned identically ("$\alpha\alpha$" stacking) in the first-stage compound.

We will present our results by quoting the energy and its components for three high-symmetry alignments of the alkali-metal and C sublattices: the metal atoms over a C hexagon, over a C—C bond, and over a C atom. The resulting crystal arrangements are shown in Fig. 7. We have chosen to study these particular points because their symmetry permits a more reliable calculation of the relative total energy at these positions. It should be noted that within the charge-density model which we use, T_{TF} and $T^{(1)}$ remain rigorously constant for the deformations which we study [Fig. 7(a)]; thus we need only recompute the variations of the Coulomb contribution and the exchange and correlation contribution to obtain relative total energies. Intuitively we expect that the lowest-energy configuration is the first of these high-symmetry points E_0 where the alkali-metal atoms sit over the centers of C

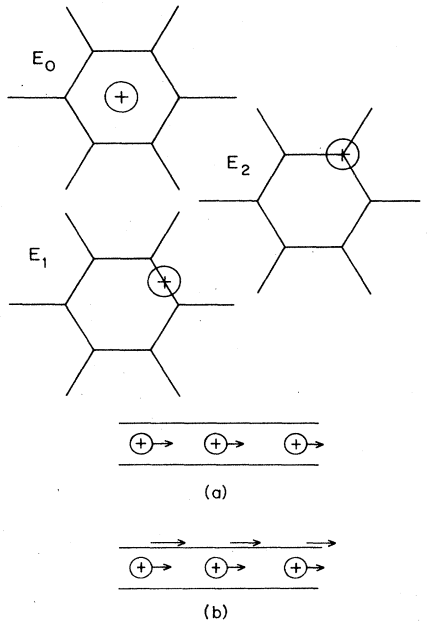

FIG. 7. (a) The three high-symmetry positions E_0, E_1, and E_2 for the alkali-metal layers with respect to the host planes for which the density-functional energies have been evaluated. Also, an edge view of the deformation studied. (b) An acoustic shear deformation. As mentioned in the text, the energies of (a) and (b) are closely related in a system without long-range forces.

hexagons; this is indeed found to be true for every alkali-metal compound studied, as shown in Table I. Furthermore, the energy above the center of a C—C bond (E_1) is always somewhat lower than the energy above a C atom (E_2). The C—C bond center is thus a saddle point for the passage of an alkali-metal atom from one hexagon center to another. Note that because we move the alkali-metal atoms rigidly, these conclusions are strictly valid only for the collective, long-wavelength motion of a group of metal atoms. We will return to a consideration of alkali-metal—alkali-metal interactions in subsection B.

Table I shows experimental results for the activation barrier E_1 as deduced from the activation energy for in-plane alkali-metal diffusion. This is determined by quasielastic neutron scattering.[9,10] The overall agreement between theory and experiment is fairly good, with the theory being consistently higher. Still, both agree that the activation energies are on the order of 1 eV for LiC_6, and on the order of 0.1 eV for the other compounds.

Previous studies of the problem of adsorbate molecules on a graphite surface[62,63] have found that the corrugations imposed by the graphite substrate are quite smoothly varying, being representable by a small number of in-plane Fourier components. By computing the total energy at a number of other low-symmetry alignments of the alkali-metal superlattice, we have determined that for the case of the intercalation compounds as well, the impurity atoms sit on an almost sinusoidal surface. This fact permits us to fit the three high-symmetry points by a sinusoidal energy function with contributions from only the six shortest reciprocal-lattice vectors of the C plane. From this fit we

may examine small harmonic excursions about the minimum point at the center of the C hexagon, relating the curvature of this minimum to the shear elastic constants of the alkali-metal–graphite compounds.

In order to associate this curvature with the shear modulus C_{44}, we must make the assumption that long-range forces between planes which are not nearest neighbors are not important; otherwise, the optic-type deformation which we are studying is not related to the acoustic distortion which determines C_{44} (see Fig. 7). While it might be thought that long-range forces are important in such a highly ionic compound, this is not the case for the distortions under study. It can be shown that an overall neutral planar structure, like a carbon-metal sandwich, interacts by an exponentially decaying force with neighboring neutral slabs;[64] thus the relevant force is short ranged. (It is therefore surprising that in recent experiments, acoustic and optic shear energetics do not seem to be simply related[65] as they should be in the nearest-neighbor force model; however, such direct experimental comparisons are rather difficult.) We have demonstrated by direct computation of the total energy for the acoustic-type distortion in Fig. 7(b) that these long-range shear forces are numerically insignificant. (Note that on the contrary, there should be and are long-ranged *compressional* forces.) Therefore we are justified in extracting C_{44} from the sinusoidal fit to our high-symmetry optic shear distortions. We have chosen not to obtain C_{44} directly from acoustic shear computations because these involve symmetry-breaking distortions of the lattice. We have found that for the extraction of these rather small energy differences, the full use of symmetry is quite important in obtaining reliable numerical estimates for the shear modulus.

Using the above assumptions, the shear modulus is obtained simply from the numbers at hand:

$$C_{44}=\frac{\pi^2}{2}\frac{E_1 c_0}{a_0^2 A_0}. \tag{15}$$

Here $a_0=2.46$ Å is the graphite lattice constant, the parameters A_0 and c_0 have been defined above, and the corrugation energy E_1 is given in Table I. The resulting estimates of the shear modulus are also given in Table I and displayed in Fig. 8. The experimental values for C_{44} are extracted in an ingenious fashion from a fit of the TA(100) branch measured by inelastic neutron scattering.[11,12] The experiment has not been performed for RbC_8 (nor of course for NaC_8). The shear elastic modulus C_{44} is about two orders of magnitude smaller than the compressional modulus C_{33}; as is well known, these compounds shear very easily. Nevertheless, we obtain reasonably good agreement between theory and experiment, especially for the heavier alkali metals. It is interesting to note that NaC_8, despite its anomalous C_{33}, has a C_{44} which is perfectly normal compared with the K, Rb, and Cs graphite intercalation compounds. Na apparently sees the C-plane corrugations just as strongly as the other heavy-alkali-metal atoms.

As for our results for C_{33}, for C_{44} we again predict that the Cs graphite intercalation compound should be slightly stiffer than the other heavy-alkali-metal graphite

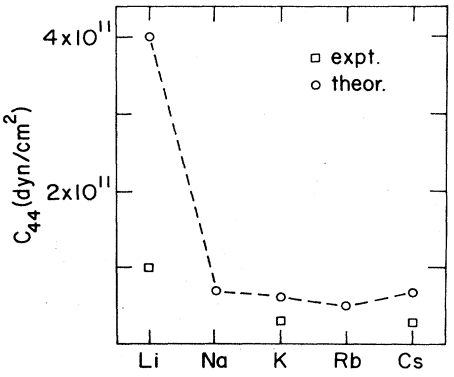

FIG. 8. Same as Fig. 6 for the shear elastic modulus C_{44}. Circles are theory, squares experiment. No experiment has been performed for RbC_8.

intercalation compounds. This seems to be borne out by experiment. The Li graphite intercalation compound continues to be quite distinct from the other alkali-metal graphite intercalation compounds, with a larger resistance to shear resulting from the more compact sandwich spacing. In our model, of course, this is directly related to the larger saddle-point barrier E_1 for Li motion. (We discuss this further below.) However, we substantially overestimate the modulus and hopping barrier for Li, certainly much more than for the heavy alkali metals. We may again take this as an indication that the simple ionic assumption for the charge density of these compounds is less reliable for Li than for the others. Still, in light of the extreme delicacy of the shear calculation, we view the agreement between theory and experiment to be quite satisfactory for all of these compounds.

Since we not only have a knowledge of the curvature of the corrugation potential near its minimum, but an essentially complete knowledge of its overall shape as well, we can relate our computations to a number of interesting physical properties which have been measured in the graphite intercalation compounds. For example, quasielastic neutron scattering[10] in the second-stage compounds RbC_{24} and CsC_{24} indicates that the alkali-metal-atom motions have both harmonic and diffusive character at room temperature. That is, the alkali atom hops to a neighboring lattice site on a significant fraction of the periods of its vibrational motion. Roughly speaking one expects this hop frequency to be simply given by a Boltzmann factor of the barrier height: $\nu_{\rm hop}\sim\nu_0\exp(-E_1/k_BT)$. With a basic phonon frequency of $\nu_0\sim10^{12}$ sec^{-1} for the heavy alkali-metal frequency, this formula gives $\nu_{\rm hop}\sim10^{10}$ sec^{-1}, using the E_1 obtained from Table I and taking T=523 K, the temperature of recent quasielastic neutron measurements.[10] This means that the alkali-metal atoms should hop very frequently, about 10^{10} times per second. This gives a diffusion coefficient[66] in the neighborhood of $D\sim a_0^2\nu_{\rm hop}\sim10^{-5}$ cm^2/sec, in rough agreement with $D=6-7\times10^{-5}$ cm^2/sec (found in Ref. 10). The comparisons made in Table I between experimental and theoretical diffusion coefficients should only be considered qualitative. For example, our analysis of D ignores the contribution from the enthalpy of alkali-

metal vacancy formation.[66,9]

For LiC_6 we see that at least in the picture presented above this hopping should be enormously less frequent, since the barrier height is about a factor of 10 higher. A recent quasielastic neutron scattering study of Li diffusion[9] in LiC_6 finds an activation energy for diffusion $E_1 \approx 0.7-1.0$ eV which is indeed much larger than that for the Rb and Cs compounds. This E_1 is qualitatively consistent with a previous estimate for the Li activation barrier as deduced from the kinetics of first-order staging transformations in Li-intercalated graphite.[3,67] These kinetics are in fact excruciatingly slow; it is found that a staging transformation takes about 200 hours at 240 K. We can work backward from this number to an estimate of the barrier height to hopping for Li atoms. It may be estimated that for the staging transformation to go to completion, Li atoms must move on the order of 1000 Å (a typical intercalant domain size). Using the standard formulas of the random walk,[68] we estimate the required number of hops N as

$$N \sim \frac{L^2}{a_0^2} = \left[\frac{1000\ \text{Å}}{2.46\ \text{Å}}\right]^2 \approx 10^5, \tag{16}$$

and the resulting hop time as

$$T \sim \frac{t_{\text{trans}}}{N} \approx \frac{200\ \text{h}}{10^5} \approx 7\ \text{sec}, \tag{17}$$

which is extremely long. We may now invert the Boltzmann factor and estimate the barrier height in LiC_6 from the observed kinetics. Taking the harmonic frequency to be $\sim 10^{12}\ \text{sec}^{-1}$, the hopping success rate is $\nu_0/\nu_{\text{hop}} = 1/\nu_{\text{hop}}T \approx 1.4\times 10^{-13}$. Therefore

$$E_1 = -k_B T \ln(1.4\times 10^{-13}) \approx 0.6\ \text{eV},\ T = 523\ \text{K}. \tag{18}$$

This estimate should be taken as extremely rough; still it is in the range of the barrier height computed using our Thomas-Fermi theory and found by the direct experiment.[9] It is somewhat smaller than our LiC_6 prediction, which is in keeping with our predicted C_{44} being too large compared with experiment. Reference 9 also obtains the diffusion constant for Li in LiC_6 at high temperatures. When extrapolated using an Arrhenius law back to $T = 523$ K, this gives $D \sim 10^{-8}\ \text{cm}^2/\text{sec}$, about three orders of magnitude lower than heavy alkali-metal diffusion constants (see Table I). An indirect confirmation of this result is given by an analysis of ^{7}Li NMR in LiC_6 (Ref. 69) which suggests that at room temperature the hop frequency defined above $\nu_{\text{hop}} \leq 3\times 10^7\ \text{sec}^{-1}$, as compared with $\nu_{\text{hop}} \sim 10^{10}\ \text{sec}^{-1}$ for the heavy alkali metals. As the table shows, our theory gives a D which is *ten* orders of magnitude smaller than for the other compounds. This error should not be taken too seriously; it is simply a result of our overestimate of E_1, combined with the extreme sensitivity of the exponential Boltzmann factor.

There is a good physical reason why our computed barrier height should constitute an upper limit on the experimentally observed barrier. This height depends strongly on the separation between C planes; it decreases rapidly as the host planes move farther apart. (In a test calculation for NaC_8, we find E_1 to vary rapidly with sandwich thickness: $dE_1/dc_0 \sim 0.1$ eV/Å.) At finite T, the C-plane separation fluctuates because of the thermal excitation of bending phonons in the graphite plane. Hopping will thus be graphite-phonon assisted, and diffusion will be increased. A possible consequence of this prediction is that the diffusion constant for Li should increase faster with T than an Arrhenius law would predict, since the effective barrier height would decrease with temperature. This deviation from Arrhenius behavior seems to be seen experimentally. Such nonactivated behavior could also be explained by the presence of two competing hopping paths for Li. Experimentally, two different hopping distances are seen in different temperature regimes. A more thorough study of the Li total-energy surface would be needed to explore these possibilities in greater detail.[9]

B. Alkali-metal-atom interactions

The above description of in-plane alkali-metal-atom energetics contains an important deficiency. As mentioned above, the above corrugation results are valid only for collective, long-wavelength motions of the alkali-metal layers; the distance between alkali-metal atoms (i.e., their average density) is taken as completely fixed. Taking Fig. 9 as our simple model for the interactions in the intercalant layer, we have determined the depth of the potential wells, but we have not obtained any information about the springs connecting the neighboring alkali-metal atoms. These springs represent an intrinsic density-dependent alkali-metal-atom—alkali-metal-atom pair interaction which is mediated by the surrounding graphite host electrons. We imagine that this interaction depends only on the in-plane averaged properties of the graphite planes, and acts independently of the graphite corrugation potential. If we can estimate these spring constants, we may then discuss additional properties of the alkali-metal

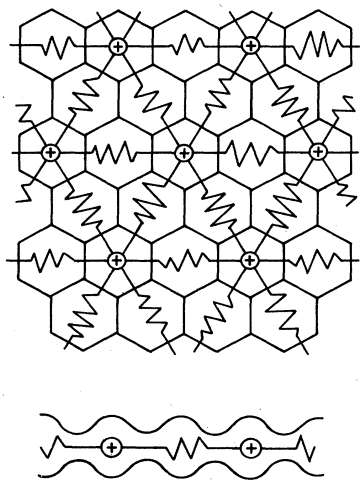

FIG. 9. Top: Schematic representation of the energetics of the intercalant layer. The alkali-metal atoms interact elastically with neighboring intercalants (the springs) and move in a potential produced by the hexagonal carbon substrate. Bottom: Side view showing the sinusoidal corrugation potential.

layers which are of current interest; the competition between commensurate and incommensurate structures, the existence and nature of domain walls, and ultimately a start on a realistic statistical mechanics of intercalant layer phases.

With these goals in mind, we have constructed an approximate procedure within our Thomas-Fermi theory for extracting these intrinsic alkali-metal—alkali-metal potentials. Motivated by the point of view that this interaction can be considered to be independent of the corrugations imposed by the graphite lattice, we use the homogeneous exponential sheet model for the graphite host developed previously.[47] This model involves replacing the real C valence charge by a model charge which is structureless in the basal plane and exponentially decaying out of the plane, and replacing the C cores by δ-function sheets of compensating charge. This simplified model is capable of accurately predicting the out-of-plane structural properties of pure graphite;[47] thus we will take it as an appropriate model for the plane-averaged properties of the C planes in the intercalation compound. To be explicit, the charge-density model which we now use for the alkali-metal—graphite compound becomes

$$\rho(r)=\sum_n \left[-\sigma_G \delta(z-nz_0)+\frac{\sigma_G+\sigma_I}{2a} e^{-|z-nz_0|/a} - \rho_c^I(r-R_n^I) \right] \tag{19}$$

This charge density is shown schematically in Fig. 10. It consists of δ-function sheets of charge representing the averaged C nuclei (with areal density σ_G), a spherically symmetric pseudoionic density representing the alkali ions (just as in the more precise calculations explained above), and homogeneous, exponentially decaying charge slabs representing the C-valence-charge density. We take the decay constant to be $a=1.23$ Å as in Ref. 47, and the areal charge density is $\sigma_G+\sigma_I$ to account for the transferred metal charge density. These simplifications to the charge density mean that many of the Coulomb parts of the total energy may be evaluated analytically; the Appendix describes these calculations in detail. We have performed extensive studies of the Li, K, Rb, and Cs first-stage alkali-metal—graphite compounds. (We do not study Na in this section.) A similar calculation of in-plane binding potentials using a "Wigner-Seitz cylinder" construction has been reported recently,[70] and new density-functional calculations of binding in pure graphite using a similar sheet approximation have been reported.[71,72] The in-plane homogeneity of the graphite charge means that we may treat the alkali-metal—alkali-metal separation a_i as a continuous variable, without being concerned with its commensurability with the graphite lattice.

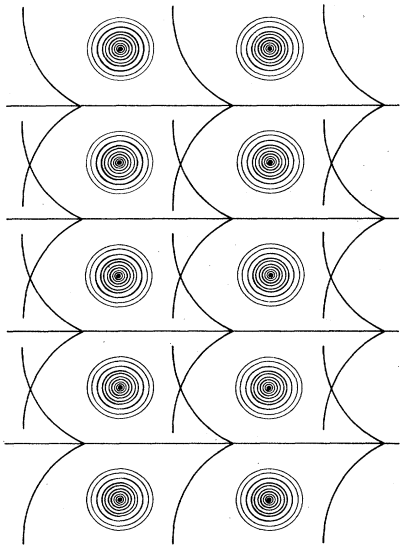

FIG. 10. Sketch of the simplified charge-density model for the intercalant compound consisting of exponentially decaying valence charges and spherically symmetric alkali-metal-ion charges.

Figures 11—14 show our results for Li, K, Rb, and Cs, respectively. The energies given are actually the energy per intercalant with the contribution from an unperturbed pure graphite unit cell of the same size subtracted out:

$$\Delta E = E_T - AE_g^0. \tag{20}$$

Here A is the area per intercalant and E_g^0 is the corresponding pure graphite energy per unit area. With this subtraction ΔE reaches a sensible, finite limit when the intercalant lattice constant is very large and the system is mostly graphite. This construction also makes the energies in Figs. 11—14 correspond to the model Coulomb energies of Ref. 73, in which the substrate energy was assumed to be zero. ΔE is the proper $T=0$ free energy describing the intercalant layer under a particular external boundary condition, namely one in which the intercalant layer is free to expand in an infinite graphite gallery and is not in contact with any external bath of intercalants.

With this in mind, we see that again an important physical difference is predicted to exist between the in-plane behavior of the alkali-metal layer in the Li graphite intercalation compound and those of the heavier alkali metals.

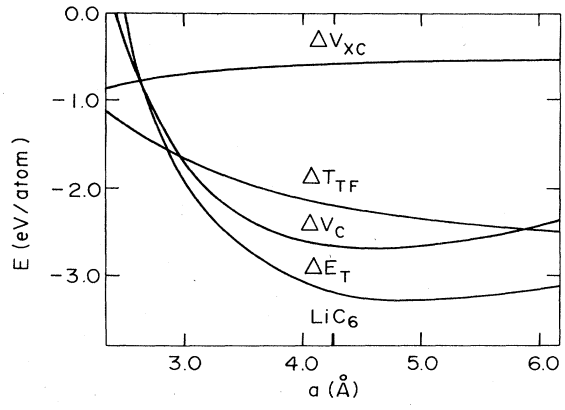

FIG. 11. Total energy ΔE_T and its various components as a function of the in-plane alkali-metal—alkali-metal separation a for first-stage lithium intercalated graphite. Energies are in eV/intercalant atom. The experimentally observed lattice constant a is indicated.

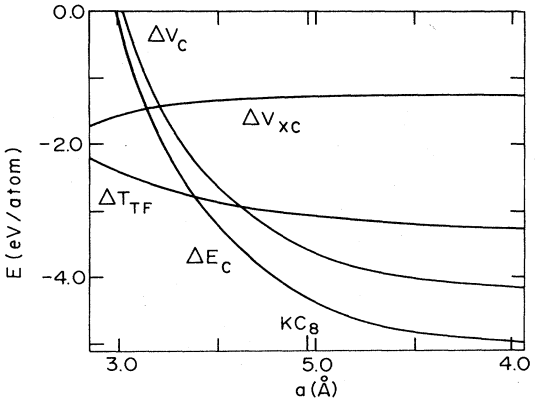

FIG. 12. Same as Fig. 11 for potassium-intercalated graphite.

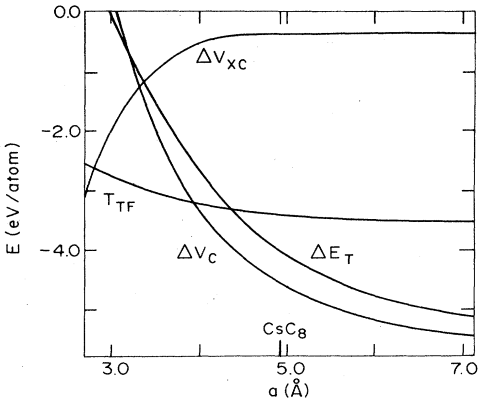

FIG. 14. Same as Fig. 11 for cesium-intercalated graphite.

While all of the total energy curves in Figs. 11—14 increase sharply at small in-plane lattice constant, the ΔE_T for Li has a minimum near the actual LiC_6 lattice constant; none of the heavier alkali metals show any minimum at all, continuing to decrease out to the largest lattice constants studied (about 50% greater than the MC_8 lattice spacing). This says that LiC_6, even in the absence of corrugation effects, should be quite stable in the absence of an external Li pressure (i.e., a chemical potential). Conversely, none of the heavier alkali-metal first-stage compounds at their observed concentrations are predicted to be stable except when immersed in a bath of alkali metal. This could have relevance for the relative vacuum stability of the first-stage alkali-metal compounds.

An examination of the individual contributions to ΔE_T reveals that this behavior has quite a simple origin and explanation. Figures 11—14 show that for each compound, the behavior of the total energy is essentially determined by its Coulomb contribution. The kinetic energy and exchange and correlation energies make only minor contributions. (The effect of the nonlinear core exchange and correlation described above is seen only in CsC_x; it is manifested as a sharp decrease in ΔE_{xc} at small alkali-metal—alkali-metal lattice constant. It has no effect at the CsC_8 concentration.) The gradient correction to the kinetic energy, in fact, is rigorously constant within the

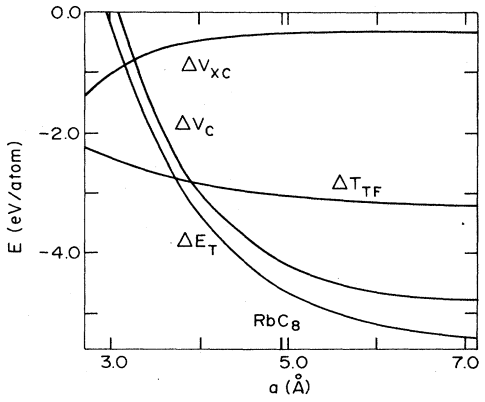

FIG. 13. Same as Fig. 11 for rubidium-intercalated graphite.

charge-density model we have used. (See the Appendix.) The presence of a minimum in the Coulomb energy for Li-intercalated graphite, which causes the minimum in the total energy, is a real effect and is precisely a manifestation of the nonmonotonic behavior of ΔV_c in a layered geometry as explained in our previous work.[73] In fact, the position of the minimum a_i relative to the layer separation c_0 in Fig. 11 agrees rather closely with the prediction of our homogeneous layer model: $a_i \approx 1.9c_0$. Actually the agreement is better than expected given the differences in the charge densities of the two models. This same rule predicts that ΔV_c for the heavier alkali metals has a minimum as well, but at a lattice constant about 80% greater than observed, and rather beyond the range of Figs. 12—14. Keep in mind, however, that our charge-density construction, in which the transferred alkali-metal-atom charge is distributed uniformly across the graphite plane, should only be reasonable for lattice constants in the same range as the in-plane screening length of the two-dimensional electron gas of the graphite plane.[52] This condition is satisfied in the vicinity of the Li minimum, but it is not in the vicinity of this extrapolated minimum for the heavier alkali metals; thus the Coulomb energy (and hence the total energy) probably remains repulsive for the heavier alkali metals at large distance. It may be that other effects (e.g., elastic) serve to stabilize the heavy alkali-metal planes at their observed density.

We can obtain more quantitative information about the intrinsic alkali-metal—alkali-metal pair potential mentioned above by fitting the curves in Figs. 11—14 about the experimentally observed equilibrium a_0. We use a quadratic fitting form

$$E(a)=3\cdot 1/2k(a-a_0)^2+G(a-a_0)+AE_g^0. \tag{21}$$

The values of the fitting constants k and G appear in Table I. The motivation for the form of Eq. (21) is that we will wish to examine the intrinsic stiffness of the alkali-metal—alkali-metal interaction, which is related to the second derivative of $E(a)$, and therefore to the fitting parameter k. We may put Eq. (21) in a more comprehensive framework by writing it as part of a free energy of a layer of intercalant with area A_T in contact with an external intercalant reservoir with chemical potential μ, and in the presence of a graphite corrugation energy V_{corr}:

$$F=\frac{A_T}{A}E(a)-N\mu+\sum_i V_{\rm corr}(\mathbf{r}_i),$$
$$=\frac{\sqrt{3}kA_T}{a^2}(a-a_0)^2+\frac{2GA_T}{\sqrt{3}a^2}(a-a_0)$$
$$+A_TE_g^0-\frac{2A_T\mu}{\sqrt{3}a^2}+\sum_i V_{\rm corr}(\mathbf{r}_i). \quad (22)$$

Here we have used $A=(\sqrt{3}/2)a^2$ (the area per intercalant), and the index i in the last term labels the positions of the intercalant atoms. We wish to connect this with the free energy for the system shown in Fig. 9, which is the canonical model for a two-dimensional system with competing periodicities:[74]

$$F_M=\frac{\sqrt{3}k_MA_T}{a^2}(a-a_0)^2+A_TE_g^0-\frac{2A_T\mu_M}{\sqrt{3}a^2}$$
$$+\sum_i V_{\rm corr}(\mathbf{r}_i). \quad (23)$$

It is clear that the only difference between Eqs. (23) and (22) is in the absence of the linear term (the term proportional to G). It is possible, however, to simultaneously redefine the spring constant and the chemical potential such that the two free energies agree near a_0 to quadratic order in the difference $(a-a_0)$. The result is

$$\mu_M=\frac{Fa_0}{2}+\mu,$$
$$k_M=k-\frac{F}{3a_0}. \quad (24)$$

This corrected spring constant k_M is of particular importance to us, and it is given in Table I. We see that the effect of the linear term is only a small correction. k_M is very similar for all of the alkali metals. This is so because the alkali-metal—alkali-metal interactions are primarily determined by the Coulomb interactions described above. These depend very little on the details of the alkali-metal pseudopotentials, arising mostly from the layered structure which is common to all the compounds.

With the free energy of Eq. (23) we can now begin to form a fairly complete picture of the equilibrium states of the intercalant layer. The (nearly sinusoidal) corrugation potential, whose height is given by E_1 in Table I, will attempt to force the intercalants into a lattice commensurate with the underlying host potential. However, if the overall intercalant concentration, as determined by the external chemical potential μ, is not a rational fraction of the host site concentration, then there will necessarily be some alkali-metal sites (either vacancies or interstitials) which are not in perfect registry with the substrate. But because of the presence of the "springs" connecting the intercalant atoms (i.e., because of the intrinsic alkali-metal-atom—alkali-metal-atom interaction) the metal lattice will relax around these mismatched sites.

If the spring constant is strong enough, this relaxation will force *all* of the atoms in the crystal out of registry with the graphite host; this lattice is referred to as "truly incommensurate" (Ref. 74). If the spring constant is somewhat weaker, most of the alkali-metal lattice will remain commensurate with the host, and the mismatch regions will organize themselves into a pattern of domain walls (also referred to as "discommensurations" or "solitons"). Such a pattern has an observable effect on diffraction patterns from such crystals, and such a discommensuration pattern has actually been inferred for stage-2 Cs-intercalated graphite.[2,8] Finally if the spring constant is very weak, the mismatch region remains disorganized and a "chaotic" pattern results.[74] The physical picture implied by Fig. 9 is somewhat related to a relaxed lattice gas model explored recently by DiCenzo.[7]

Using the data collected in Table I we may estimate to which of these three regimes the first-stage intercalation compounds belong. The free energy of Eq. (24) is the two-dimensional analog to the well-known Frank and van der Merwe energy in one dimension.[74] This model is known to possess all three regimes. Furthermore, an estimate exists for the soliton or domain-wall width in this model. In our notation, this width l_0 is (at zero temperature)

$$l_0\approx\frac{a_0^2}{2}\left[\frac{2k_M}{\Delta E}\right]^{1/2}. \quad (25)$$

If this width l_0 is less than or on the same order as the particle separation, then the system is in the chaotic regime. l_0 on the order of a few lattice constants indicates that the system contains well-organized solitons. Very large l_0 is a signal for incommensurate behavior. We believe that it is quite reasonable to apply the formula of Eq. (25) to the present two-dimensional case, at least for qualitative purposes. The resulting l_0 for LiC_6, KC_8, RbC_8, and CsC_8 are given in Table I.

Again the Li graphite intercalation compound is distinct from the others. The elastic constants k_M are all in roughly the same neighborhood for all of the compounds; however, because of its quite large corrugation height, the domain-wall width in LiC_6 is quite small, on the order of the Li-Li spacing. The heavier alkali-metal graphite intercalation compounds have a smaller corrugation and hence an l_0 which extends over about five lattice constants. These results are consistent with the Li graphite intercalation compound containing no well-organized domain-wall structure, with such structure being possible in the heavier alkali metals. Experimentally no domain structure has been seen in the Li graphite intercalation compounds[4] (although it seems that no careful search has been made), while these domain walls have been deduced from diffraction studies of CsC_{24} (Ref. 8). In fact, recent modeling of these systems using a Landau free energy[75] seems to demonstrate conclusively that these compounds do display a honeycomb domain-wall structure.

Our conclusions are thus generally consistent with the existing experiment. However, we would like to point out that Refs. 8 and 76 find domain wall widths significantly narrower than predicted above, calling into question the quantitative accuracy of Eq. (25). The recent Landau theory of these materials,[75] although quite successful, cannot predict the shape of the domain walls; more input from microscopic theory is required. We note that our results are also consistent with the presently held view[77,57]

that at *elevated* temperatures (i.e., $k_B T > E_1$), the Cs layers (and presumably those of the other heavy alkali metals) form a classic, positionally disordered two-dimensional liquid. Thus the picture is that a large fraction of the alkali-metal atoms sit in registry with the carbon lattice in the low-temperature phase because of the moderate size of l_0, but can become unregistered at high temperature. This could explain the recent observation[78] of a large jump in the shear modulus C_{44} upon going from the high-temperature disordered phase in KC_{24} or RbC_{24} to the low-temperature ordered phase. In our model, contributions to C_{44} come only from registered atoms sitting near the center of carbon hexagons. We might further predict the disordered phase of Li-intercalated graphite will be of a lattice-liquid type,[79,9] so that no large jump in C_{44} should occur at the order-disorder phase transition.[79] We have already used a strong-corrugation model for Li-intercalated graphite to explain the overall features of its $T-x$ (Ref. 14) and $T-p$ (Ref. 3) phase diagrams.

IV. CONCLUSIONS

We have developed a manageable theory for the structural properties of the graphite intercalation compounds. The results presented here should contribute to an understanding of some phenomena of current interest. For instance, our finding that the corrugation energy of the graphite host is of large magnitude in the alkali-metal intercalation compounds suggests an explanation for the observed long equilibration times in these materials. Such corrugation effects should be considered and included in studies on the formation of nonequilibrium domain structure.[80]

There are a number of simple extensions of the present work which might be considered in the future. Density-functional studies could be performed on higher-stage compounds. Model studies[81] suggest that the alkali-metal graphite interactions are very nearly stage independent; it would be interesting to check this result using a more microscopic theory. The ternary alkali-metal compounds (e.g., $K_{1-x}Rb_xC_8$) still present an unsolved theoretical problem with their dramatic elastic and magnetic anomalies as a function of composition.[82] A suggestion that an anomaly may occur in the charge transfer as a function of composition has not received experimental support.[83] Finally, it is possible that a form of Thomas-Fermi theory could be applied to the acceptor intercalation compounds. This is an area for which fundamental theory is almost totally lacking, for which an immense variety of interesting structural phenomena have been reported.[2] Studies of domain structures in these materials remain very active.[84]

To summarize, we have performed structural energy calculations for the alkali-metal graphite intercalation compounds. The simplicity of our formalism permits a comprehensive investigation of a wide variety of properties, including lattice constants, elastic moduli, alkali-metal atom diffusion constants, activation energies, and domain-wall widths. Interplane interactions are dominated by classical Coulomb attraction between charged layers and hard-ion repulsion. The Li ion is much smaller than those of the heavy alkali metals, which explains the smaller lattice constant and large elastic moduli of the Li graphite intercalation compound. The Na—C interaction is found to be anomalously weak. The alkali-metal intraplane interaction is dominated almost entirely by Coulomb interactions, and is essentially the same for all the alkali metals.

ACKNOWLEDGMENTS

This work was supported by the National Science Foundation—Materials Research Laboratory program under Grant No. DMR-82-16718. One of us (E.J.M.) is grateful for the support from the A. P. Sloan Foundation.

APPENDIX

In this appendix we present closed-form results for the Coulomb energy pieces of the Thomas-Fermi energy functional [Eq. (1)] for the simple charge-density model for the first-stage alkali-metal graphite intercalation compounds of Eq. (19). To repeat this equation, the model charge is given by

$$\rho(r)=\sum_n \left[-\sigma_G \delta(z-nz_0)+\frac{\sigma_G+\sigma_I}{2a}\exp(-|z-nz_0|/a) - \rho_c^I(r-R_n^I) \right]$$

$$=\rho_{\text{sheet}}+\rho_{\text{expo}}+\rho_c^I. \tag{A1}$$

The notation is self-explanatory. Unfortunately it is not possible to obtain a fully analytical expression for this Coulomb energy as we can for pure graphite.[47] Still, many of its components can be computed analytically. Following a standard procedure,[47] we add and subtract charge densities in order to obtain separately neutral densities:

$$\rho(r)=(\rho_{\text{sheet}}+\bar{\rho}_G)+(\rho_{\text{expo}}-\bar{\rho}_T) +(\rho_c^I-\rho_{\text{points}}^I)+(\rho_{\text{points}}^I-\bar{\rho}_G)$$

$$=\rho_1+\rho_2+\rho_3+\rho_4. \tag{A2}$$

Here $\bar{\rho}_{G,I,T}$ are the appropriate uniform charge densities and ρ_{points}^I represents a lattice of point charges $-Z_i^I$ placed at the intercalant sites. We compute the total Coulomb energy in parts:

$$V_C=V_C^{11}+V_C^{22}+V_C^{33}+V_C^{44}+2V_C^{12} +2V_C^{13}+2V_C^{14}+2V_C^{23}+2V_C^{24}+2V_C^{34}. \tag{A3}$$

Here

$$V_C^{ij}\equiv\int_\Omega\int_\Omega \frac{\rho_i(\mathbf{r}_1)\rho_j(\mathbf{r}_2)}{|\mathbf{r}_1-\mathbf{r}_2|}d\mathbf{r}_1 d\mathbf{r}_2. \tag{A4}$$

The pieces of the sum in Eq. (A3) which must be computed numerically are as follows:

(1) V_C^{44}. This is simply the energy of point charges in jellium, and is computed by an Ewald summation.[85]

(2) $V_C^{13}+V_C^{14}$. This can be done numerically by a single one-dimensional integral in real space.

(3) $V_C^{23}+V_C^{24}$. This, the interaction of the smooth exponentials with the intercalant ionic potentials, is done as a sum in G space.[47] It is possible to perform it as an r space integral as well.

The remainder of the Coulomb energy components may be evaluated analytically. The results are

$$V_C^{11}=\frac{\pi\Omega_0\sigma_G^2}{3}, \tag{A5}$$

$$2V_C^{12}=2\pi a A_0\sigma_T\sigma_G\left[2\coth\beta-\frac{2}{\beta}-\frac{2}{3}\beta\right], \tag{A6}$$

$$2V_C^{14}=-\frac{\pi\Omega_0\sigma_G Z_i^I}{3A_0}, \tag{A7}$$

$$V_C^{22}=8\pi a A_0\sigma_T^2\left[-\frac{3}{8}\coth\beta+\frac{1}{2\beta}+\frac{1}{12}\beta-\frac{1}{8}\beta\frac{1}{\sinh^2\beta}\right]. \tag{A8}$$

V_C^{33} is not computed since it is density independent. Use of these analytic expressions considerably speeds the computation of the in-plane alkali-metal potentials (Figs. 11–14). As for the other components of the total energy, the exchange and correlation piece requires a full three-dimensional integration [done by fast Fourier transform (FFT) techniques]; the Thomas-Fermi kinetic energy requires just a one-dimensional integral as for pure graphite; and the gradient correction need not be computed at all since it does not depend on the basal-plane area per intercalant A_0 and so remains rigorously constant as the in-plane lattice constant changes.

*Present address: Laboratory of Atomic and Solid State Physics and Materials Science Center, Cornell University, Ithaca, NY 14853.

[1]M. S. Dresselhaus and G. Dresselhaus, Adv. Phys., **30**, 139 (1981).
[2]R. Clarke and C. Uher, Adv. Phys. **33**, 469 (1984).
[3]D. P. DiVincenzo, C. D. Fuerst, and J. E. Fischer, Phys. Rev. B **29**, 1115 (1984).
[4]K. C. Woo, W. A. Kamitakahara, D. P. DiVincenzo, D. G. Robinson, H. Mertwoy, J. W. Milliken, and J. E. Fischer, Phys. Rev. Lett. **50**, 182 (1983).
[5]R. Clarke, N. Wada, and S. A. Solin, Phys. Rev. Lett. **44**, 1616 (1980); N. Wada, Phys. Rev. B **24**, 1065 (1981); N. Wada, R. Clarke, and S. A. Solin, Solid State Commun. **35**, 675 (1980).
[6]C. Horie, S. A. Solin, H. Miyazaki, S. Igarashi, and S. Hatakeyama, Phys. Rev. B **27**, 3796 (1983).
[7]S. B. DiCenzo, Phys. Rev. B **26**, 5878 (1982).
[8]R. Clarke, J. N. Gray, H. Homma, and M. J. Winokur, Phys. Rev. Lett. **47**, 1407 (1981); M. B. Gordon, J. Villain, and R. Clarke, Phys. Rev. B **25**, 7871 (1982).
[9]H. Zabel (unpublished); A. Magerl, H. Zabel, and I. S. Anderson (unpublished).
[10]H. Zabel, A. Magerl, A. J. Dianoux, and J. J. Rush, Phys. Rev. Lett. **50**, 2094 (1983).
[11]H. Zabel, A. Magerl, and J. J. Rush, Phys. Rev. B **27**, 3930 (1983).
[12]H. Zabel, W. A. Kamitakahara, and R. M. Nicklow, Phys. Rev. B **26**, 5919 (1982).
[13]H. Zabel and A. Magerl, Phys. Rev. B **25**, 2463 (1982).
[14]D. P. DiVincenzo and T. C. Koch, Phys. Rev. B **30**, 7092 (1984).
[15]S. A. Safran, Phys. Rev. Lett. **44**, 937 (1980); Synth. Met. **2**, 1 (1980).
[16]S. A. Safran and D. R. Hamann, Phys. Rev. B **23**, 565 (1981); **22**, 606 (1980).
[17]S. E. Millman and G. Kirczenow, Phys. Rev. B **26**, 2310 (1982).
[18]J. R. Dahn, D. C. Dahn, and R. R. Haering, Solid State Commun. **42**, 179 (1982).
[19]S. E. Millman and G. Kirczenow, Phys. Rev. B **28**, 3482 (1983); S. E. Millman, G. Kirczenow, and D. Solenberger, J. Phys. C **15**, L1269 (1982).
[20]P. Hawrylak and K. R. Subbaswamy, Phys. Rev. B **28**, 4851 (1983).
[21]G. Kirczenow, Phys. Rev. Lett. **52**, 437 (1984).
[22]P. Hohenberg and W. Kohn, Phys. Rev. **136**, B864 (1964).
[23]W. Kohn and L. J. Sham, Phys. Rev. **140**, A1133 (1965).
[24]V. L. Moruzzi, J. F. Janak, and A. R. Williams, *Calculated Electronic Properties of Metals* (Pergamon, New York, 1978).
[25]M. T. Yin and M. L. Cohen, Phys. Rev. B **25**, 4317 (1982), and references therein.
[26]N. A. W. Holzwarth, S. G. Louie, and S. Rabii, Phys. Rev. B **28**, 1013 (1983); N. A. W. Holzwarth, S. Rabii, and L. A. Girifalco, *ibid.* **18**, 5190 (1978); N. A. W. Holzwarth, L. A. Girifalco, and S. Rabii, *ibid.* **18**, 5206 (1978).
[27]D. P. DiVincenzo and S. Rabii, Phys. Rev. B **25**, 411 (1982).
[28]R. C. Tatar and S. Rabii (unpublished).
[29]N. A. W. Holzwarth, D. P. DiVincenzo, R. C. Tatar, and S. Rabii, Int. J. Quantum Chem. **23**, 1223 (1983).
[30]M. Weinert, E. Wimmer, and A. J. Freeman, Phys. Rev. B **26**, 4571 (1982); M. Posternak, A. Baldereschi, A. J. Freeman, and E. Wimmer, Phys. Rev. Lett. **52**, 863 (1984).
[31]N. H. March, in *Theory of the Inhomogeneous Electron Gas*, edited by S. Lundqvist and N. H. March (Plenum, New York, 1983), p. 1.
[32]C. Muhlhausen and R. G. Gordon, Phys. Rev. B **24**, 2147 (1981); **24**, 2161 (1981); J. R. Chelikowsky, Phys. Rev. Lett. **47**, 387 (1981).
[33]T. Ohno, N. Nakao, and H. Kamimura, J. Phys. Soc. Jpn. **47**, 1125 (1979).
[34]M. E Preil and J. E. Fischer, Phys. Rev. Lett. **52**, 1141 (1984).
[35]J. J. Ritsko and C. F. Brucker, Solid State Commun. **44**, 889 (1982).
[36]D. Billaud, A. Hérold, and F. L. Vogel, Synth. Met. **3**, 279 (1981).
[37]M.-C. Robert-Picard, M. Oberlin, and J. Méring, C. R. Acad. Sci., Ser. C **266**, 1043 (1968).
[38]R. C. Asher and S. A. Wilson, Nature (London) **181**, 409 (1958).
[39]D. P. DiVincenzo and E. J. Mele, Phys. Rev. Lett. **53**, 52

(1984); **53**, 742(E) (1984).
[40]D. P. DiVincenzo and E. J. Mele, in *Intercalated Graphite,* edited by M. S. Dresselhaus, G. Dresselhaus, J. E. Fischer, and M. J. Moran (North-Holland, New York, 1983), p. 123.
[41]J. C. Slater, Phys. Rev. **51**, 846 (1937).
[42]D. M. Ceperly and B. J. Alder, Phys. Rev. B **23**, 5048 (1981).
[43]L. Hedin and B. I. Lundqvist, J. Phys. C **4**, 2664 (1971).
[44]J. P. Perdew and A. Zunger, Phys. Rev. B **23**, 5048 (1981).
[45]For example, M. S. Hybertson and S. G. Louie, Solid State Commun. **51**, 451 (1984).
[46]C. Q. Ma and V. Sahni, Phys. Rev. B **16**, 4249 (1977).
[47]D. P. DiVincenzo, E. J. Mele, and N. A. W. Holzwarth, Phys. Rev. **27**, 2458 (1983).
[48]J. Ihm, A. Zunger, and M. L. Cohen, J. Phys. C **12**, 4409 (1979); **13**, 3095(E) (1980).
[49]D. R. Hamann, M. Schlüter, and C. Chiang, Phys. Rev. Lett. **43**, 1494 (1979).
[50]G. P. Kerker, J. Phys. C **13**, L189 (1980).
[51]S. G. Louie, S. Froyen, and M. L. Cohen, Phys. Rev. B **26**, 1738 (1982).
[52]D. P. DiVincenzo and E. J. Mele, Phys. Rev. B **29**, 1685 (1984).
[53]G. R. Hennig, in *Proceedings of the First and Second International Conferences on Carbon* (University of Buffalo, Buffalo, 1956), p. 103.
[54]F. Herman and S. Skillman, *Atomic Structure Calculations* (Prentice-Hall, Englewood Cliffs, N. J., 1963).
[55]G. B. Bachelet, D. R. Hamann, and M. Schlüter, Phys. Rev. B **26**, 4199 (1982).
[56]J. H. Rose, J. R. Smith, and J. Ferrante, Phys. Rev. B **28**, 1835 (1983).
[57]S. A. Solin, Adv. Chem. Phys. **49**, 455 (1982).
[58]J. E. Fischer, Mater. Sci. Eng. **31**, 211 (1977).
[59]M. Y. Chou, S. G. Louie, M. L. Cohen, and N. A. W. Holzwarth, Phys. Rev. B **30**, 1062 (1984).
[60]G. Loupias, J. Chomilier, and D. Guérard, J. Phys. (Paris) Lett. **45**, L301 (1984).
[61]C. Kittel, *Introduction to Solid State Physics,* 3rd ed. (Wiley, New York, 1967), p. 98.
[62]M. W. Cole, D. R. Frankl, and D. L. Goodstein, Rev. Mod. Phys. **53**, 199 (1981); R. B. Laughlin, Phys. Rev. B **25**, 2222 (1982).
[63]D. L. Freeman, J. Chem. Phys. **62**, 941 (1975).
[64]We thank Dr. D. Vanderbilt for pointing this out to us.
[65]W. A. Kamitakahara, private communication.
[66]L. A. Girifalco, *Statistical Physics of Materials* (Wiley, New York, 1973), p. 256.
[67]D. P. DiVincenzo, Ph.D. thesis, University of Pennsylvania, 1983 (unpublished).
[68]L. E. Reichl, *A Modern Course in Statistical Physics* (University of Texas, Austin, 1980), p. 151.
[69]C. J. Conard and H. Estrade, Mater. Sci. Eng. **31**, 173 (1977).
[70]H. Miyazaki, Y. Kuramoto, and C. Horie, J. Phys. Soc. Jpn. **53**, 1380 (1984).
[71]M. Leal and E. Santos, Nuovo Cimento **1D**, 716 (1982).
[72]E. Santos and A. Villagrá, Phys. Rev. B **6**, 3134 (1972); E. Gaite, M. Leal, and E. Santos, Phys. Rev. B **31**, 8226 (1985).
[73]D. P. DiVincenzo and E. J. Mele, Phys. Rev. B **25**, 7822 (1982).
[74]P. Bak, Rep. Prog. Phys. **45**, 587 (1982); F. C. Frank and J. H. van der Merwe, Proc. R. Soc. London **198**, 205 (1949).
[75]M. Suzuki and H. Suematsu, J. Phys. Soc. J. **52**, 2761 (1983).
[76]N. Caswell, S. A. Solin, T.M. Hayes, and S. J. Hunter, Physica (Utrecht) **99B**, 463 (1980).
[77]M. Plischke, Can. J. Phys. **59**, 802 (1981).
[78]S. E. Hardcastle, D. A. Neumann, H. Zabel, and J. J. Rush (unpublished).
[79]J. Rossat-Mignod, A. Wiedenmann, K. C. Woo, J. W. Milliken, and J. E. Fischer, Solid State Commun. **44**, 1339 (1982); D. S. Robinson and M. B. Salamon, Phys. Rev. Lett. **48**, 156 (1982).
[80]P. Hawrylak and K. R. Subbaswamy, Phys. Rev. Lett. **53**, 2098 (1984).
[81]R. Al-Jishi and G. Dresselhaus, Phys. Rev. B **26**, 4523 (1982).
[82]D. A. Neumann, H. Zabel, J. J. Rush, and N. Berk, Phys. Rev. Lett. **53**, 56 (1984).
[83]P. C. Chow, D. A. Neumann, D. G. Wiesler, H. Zabel, and S. B. DiCenzo (unpublished).
[84]D. M. Hwang, X. W. Qian, and S. A. Solin, Phys. Rev. Lett. **53**, 1473 (1984).
[85]W. A. Harrison, *Pseudopotentials in the Theory of Metals* (Benjamin, New York, 1966), p.166; K. Fuchs, Proc. R. Soc. London, Ser. A **151**, 585 (1935).